Supporting Information

Tannic acid-modified polyvinyl alcohol hydrogel electrolyte enabling dendrite-free and flexible aqueous zinc-ion batteries

Lixin Wang[a], Yan Shi[a]*, Daliang Han[b], Yi Gong[c], Long Li[a], Xiaoning Tang[a], Huanxin Li[d]*, Jiaojing Shao[a]*

[a]College of Materials and Metallurgy, Guizhou University, Guiyang 550025, China. E-mail: yshi3@gzu.edu.cn, shiyan1262006@126.com; xjshao@gzu.edu.cn

[b]Nanoyang Group, Tianjin Key Laboratory of Advanced Carbon and Electrochemical Energy Storage, School of Chemical Engineering and Technology, Tianjin University, Tianjin 300072, China

[c]Department of Chemical Engineering, Imperial College London, London SW7 2AZ, UK

[d]Department of Chemical Engineering, University College London, London WC1E 7JE, UK. E-mail: huanxin.li@ucl.ac.uk

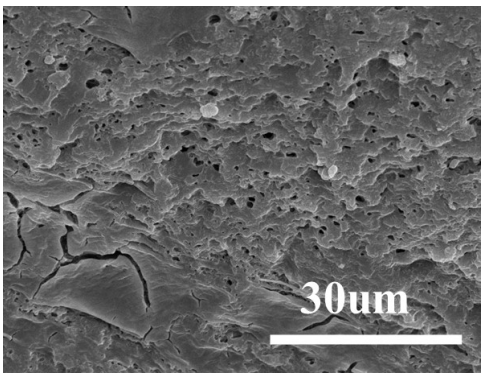

Fig. S1 Surface morphology of the pure PVA hydrogel electrolyte.

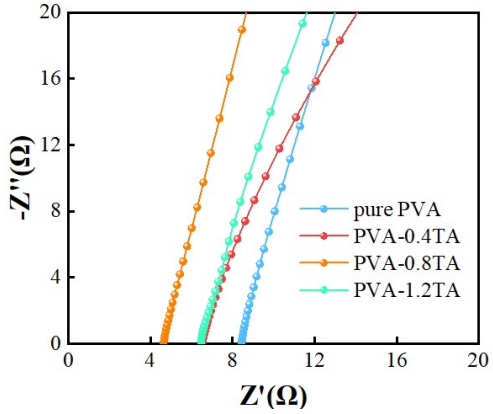

Fig. S2 Nyquist plots of the hydrogel electrolytes.

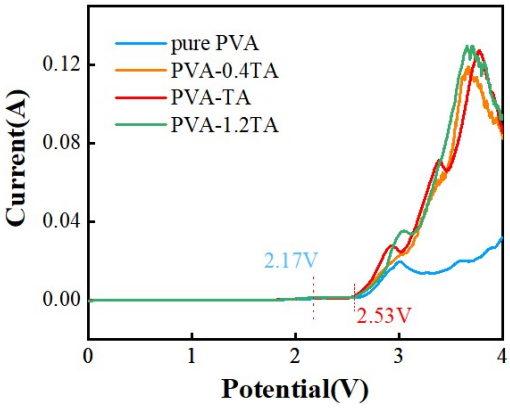

Fig. S3 LSV curves of the hydrogel electrolytes with different components.

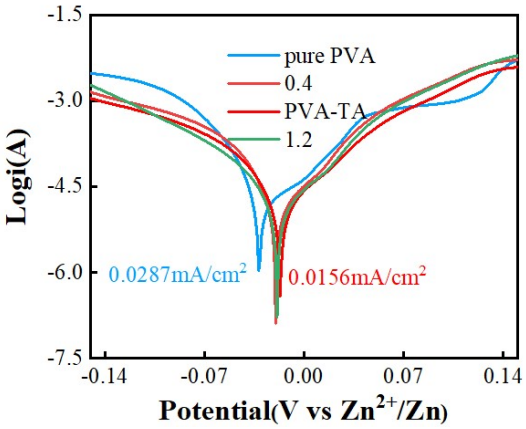

Fig. S4 Tafel plots of the hydrogel electrolytes with different components.

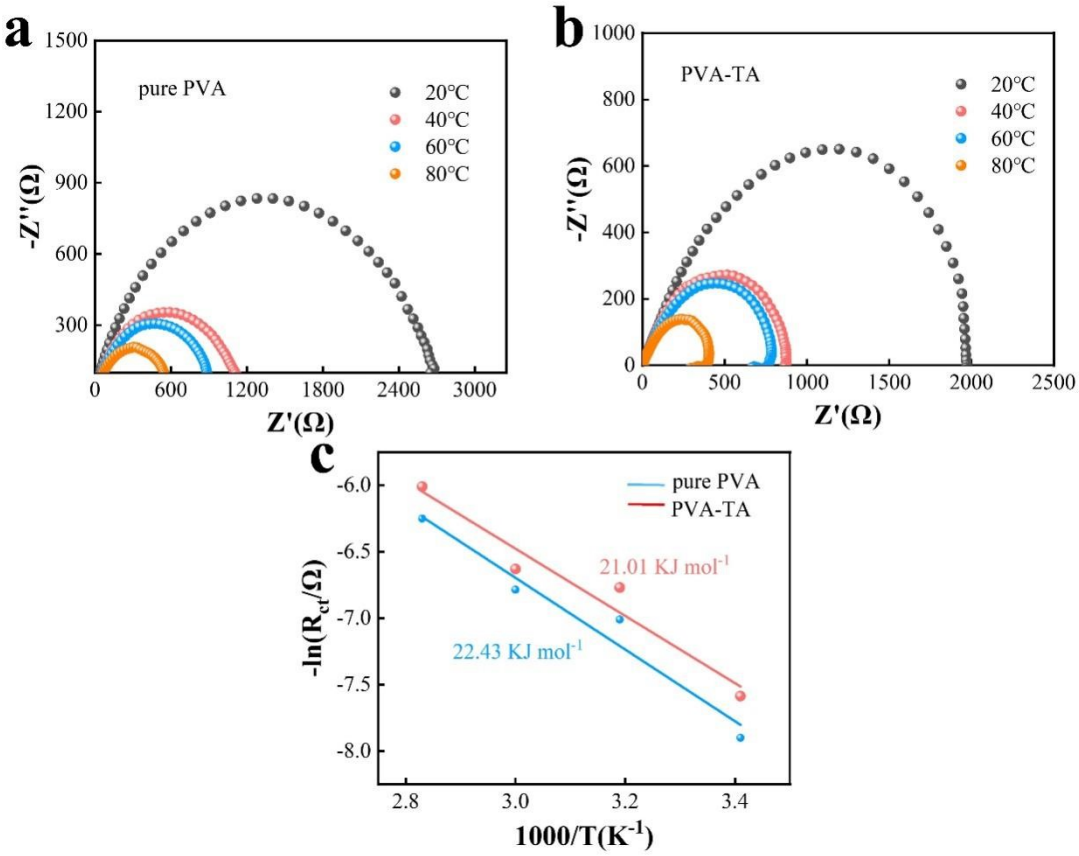

Fig. S5 Rct values of the hydrogel electrolytes measured at different temperatures and Arrhenius plots and corresponding activation energies for Zn^{2+} conduction.

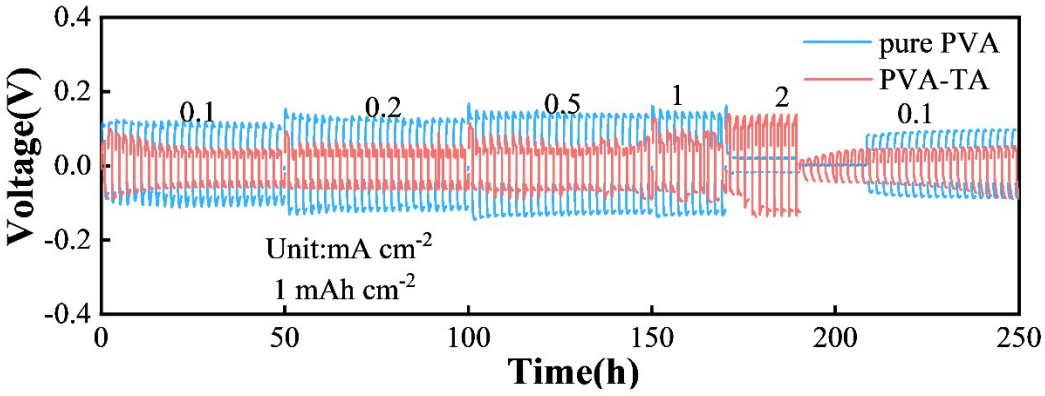

Fig. S6 Cycle Stability of PVA-Based Hydrogel Electrolytes at Different Current Densities.

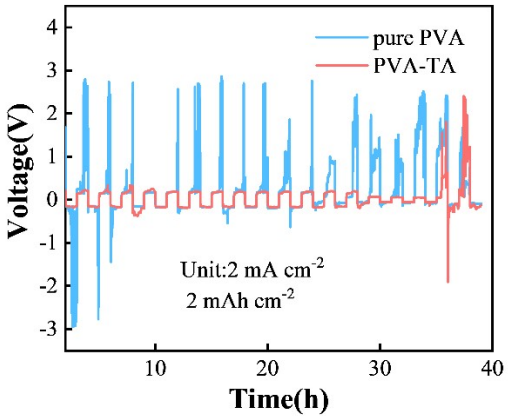

Fig. S7 Cycling stability at 2 mA cm^{-2}.

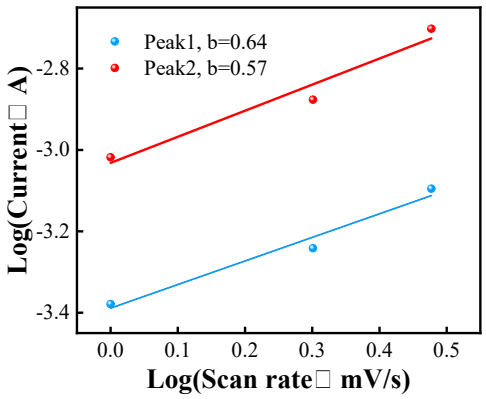

Fig. S8 Log-log plots of peak currents versus sweep rates derived from CV measurements.

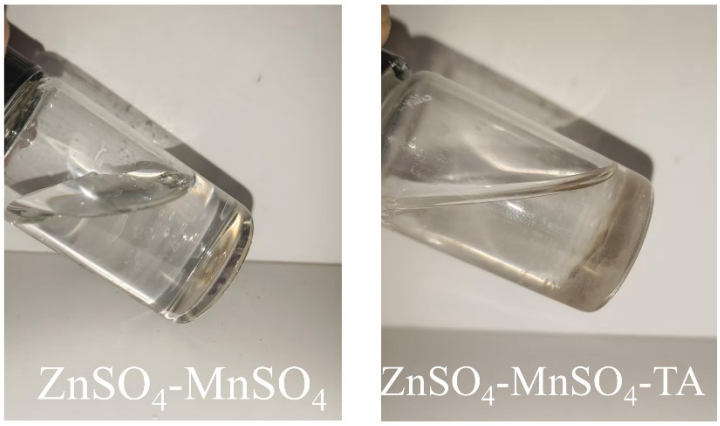

Fig. S9 Images of $ZnSO_4$-$MnSO_4$ and $ZnSO_4$-$MnSO_4$-TA electrolytes.

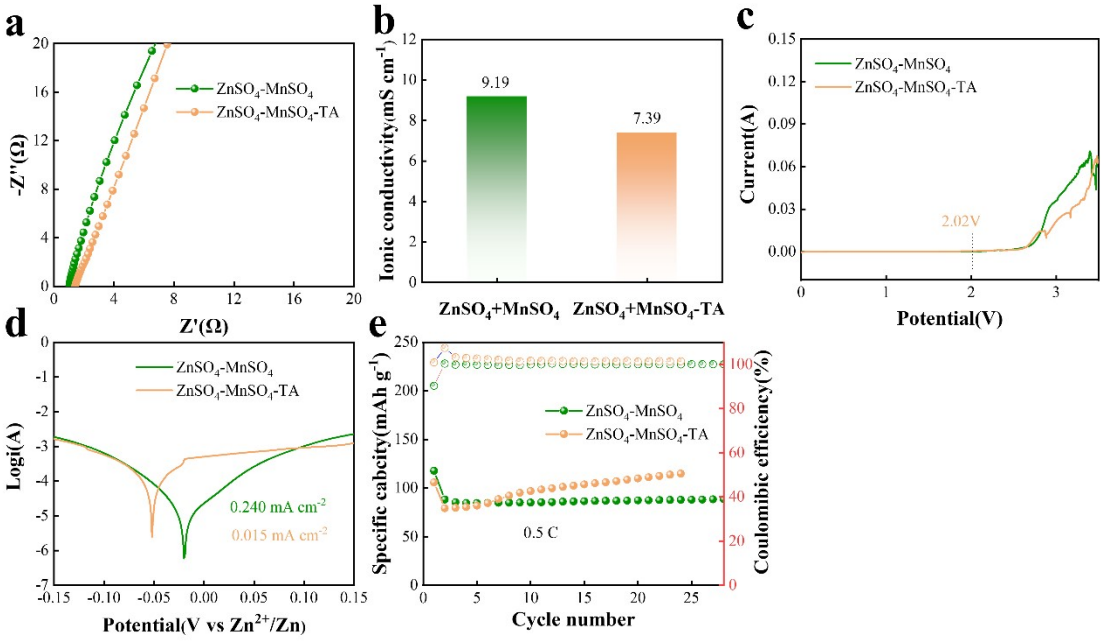

Fig. S10 Electrochemical performance of $ZnSO_4$-$MnSO_4$ and $ZnSO_4$-$MnSO_4$-TA electrolytes, and cycling performance of the assembled Zn||MnO_2 batteries. (a) Nyquist plots of the hydrogel electrolytes. (b) Ionic conductivity of the hydrogels. (c) Linear sweep voltammetry (LSV) curves. (d) Tafel plots of Zn||Zn symmetric cell using the different hydrogel electrolytes. (e) Cycle performance at 0.5 C.

Batteries assembled with commercial PP separators were used to test the electrochemical and battery performance of $ZnSO_4$-$MnSO_4$ and $ZnSO_4$-$MnSO_4$-TA

electrolytes. As shown in Fig S10, the complexation of TA with Zn^{2+} reduces the effective concentration of free Zn^{2+} ions. Zn‖MnO_2 batteries containing the TA-based electrolyte exhibited poorer cycling performance than those with the pure $ZnSO_4$-$MnSO_4$ electrolyte. These results clearly demonstrate that simply adding TA to $ZnSO_4$-$MnSO_4$ does not improve battery performance; instead, it leads to degradation. Therefore, the performance enhancement is indeed attributable to the complete PVA-TA electrolyte system rather than the TA molecule alone.

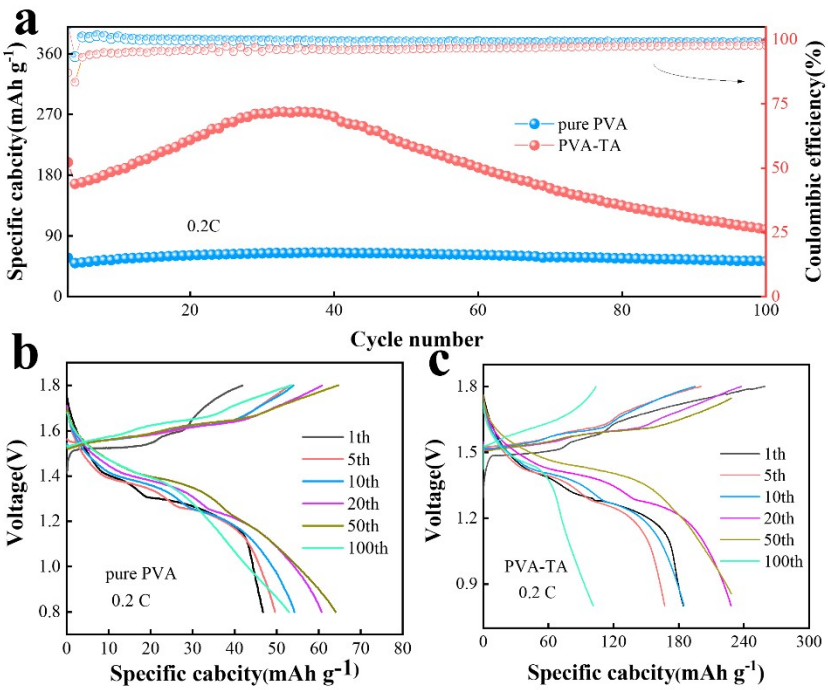

Fig. S11 Cycle performance at 0.2 C, (b) and (c) charge-discharge profiles over different cycles for full cell.

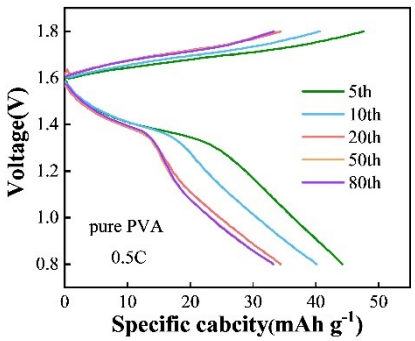

Fig. S12 Charge-discharge profiles over different cycles for Zn||PVA||MnO_2 cell.

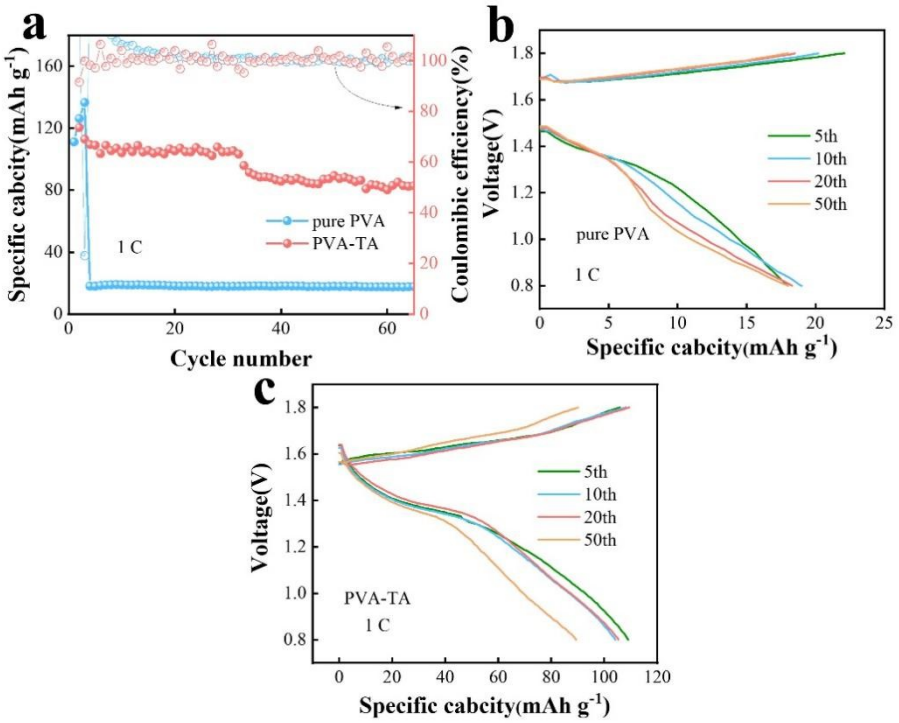

Fig. S13 Cycle performance at 1 C, (b) and (c) charge-discharge profiles over different cycles for full cell.